Published in final edited form as:
Dev Dyn. 2010 August ; 239(8): 2190–2197. doi:10.1002/dvdy.22355.

Oda16/Wdr69 is essential for axonemal dynein assembly and ciliary motility during zebrafish embryogenesis

Chunlei Gao, **Guangliang Wang**, **Jeffrey D. Amack**, and **David R. Mitchell**
State University of New York Upstate Medical University, Department of Cell and Developmental Biology

Abstract

In the alga C*hlamydomonas reinhardtii*, Oda16 functions during ciliary assembly as an adaptor for intraflagellar transport of outer arm dynein. Oda16 orthologs only occur in genomes of organisms that use motile cilia, however, such cilia play multiple roles during vertebrate development and the contribution of Oda16 to their assembly remains unexplored. We demonstrate that the zebrafish Oda16 ortholog (Wdr69) is expressed in organs with motile cilia and retains a role in dynein assembly. Antisense morpholino knockdown of Wdr69 disrupts ciliary motility and results in multiple phenotypes associated with vertebrate ciliopathies. Affected cilia included those in Kupffer's vesicle, where Wdr69 plays a role in generation of asymmetric fluid flow and establishment of organ laterality, and otic vesicles, where Wdr69 is needed to develop normal numbers of otoliths. Analysis of cilium ultrastructure revealed loss of outer dynein arms in morphant embryos. These results support a remarkable level of functional conservation for Oda16/Wdr69.

Keywords

cilia; asymmetry; intraflagellar transport; axonemal dynein; *situs inversus*

Introduction

Ciliopathies, disorders caused by cilia malfunction, include defects related to both motile and non-motile cilia. Non-motile cilia, present on nearly all vertebrate cells, serve as sensory organelles and their dysfunction leads to the onset of a wide range of disorders including polycystic kidney disease (PKD). Functions of motile cilia/flagella include clearing airways, circulating cerebrospinal fluid and facilitating fertilization, and their absence or dysfunction leads to disorders categorized as primary ciliary dyskinesia (PCD) (Eley et al., 2005). In addition, cilia are now recognized to play a number of roles during embryo development. For example, motile cilia on the node of the mouse embryo generate a leftward fluid flow that initiates the establishment of embryonic left-right asymmetry (Nonaka et al., 1998; Okada et al., 2005), and about half of human PCD patients display *situs inversus*, a defect in left-right asymmetry of internal organs. Ultrastructural analyses of cilia from PCD patients reveal various defects in the normal 9 + 2 ciliary composition, including loss of central pair microtubules, radial spokes, and dynein arms. The most often found defect is loss of outer arm dynein, one of the ATPases that power ciliary bending (Olbrich et al., 2002; Carlen and Stenram 2005).

Corresponding author: David R. Mitchell, SUNY Upstate Medical University, Department of Cell and Developmental Biology, 750 E Adams St., Syracuse, NY, 13210, USA, Phone: 315-464-8575, FAX: 315-464-8535, mitcheld@upstate.edu.

To better understand the range of mutations that can lead to defects in axonemal dynein assembly and cause PCD, we have been analyzing dynein assembly mutations in *Chlamydomonas reinhardtii*, a single-celled green alga that contains two flagella, which structurally and functionally resemble cilia and which display both motile and sensory functions. One such mutation, *oda16*, selected in a screen for *Chlamydomonas* proteins involved in outer dynein arm assembly, was characterized as an intraflagellar transport (IFT) adaptor needed for normal assembly of outer arm dyneins in this organism (Ahmed and Mitchell 2005; Ahmed et al., 2008). This function is unique among dynein assembly defects, and thus far represents the only example of an IFT-associated protein that plays an essential role in assembly of a specific axonemal cargo. For comparison, most dynein assembly defects are mutations in dynein ATPase subunits and not in IFT-associated proteins, and most mutations in IFT proteins, such as IFT88 (Pazour et al., 2000), completely disrupt ciliary assembly rather than creating cargo-specific defects. Homologs of Oda16, a WD repeat protein (WDR69 in humans), are only found in organisms that retain motile cilia, suggesting that Oda16 retains a function in axonemal dynein assembly (Ahmed and Mitchell 2005; Ahmed et al., 2008), despite the evolutionary distance between green algae and vertebrates. However, no mutations have been identified that disrupt Oda16 homologs in organisms other than *Chlamydomonas*, and recent experiments with other conserved genes involved in axonemal dynein assembly have not always supported a universally conserved assembly mechanism for these large ATPase complexes. In the case of mutations affecting PF13/Ktu, similar disruption of both inner and outer row dynein assembly was observed in *Chlamydomonas*, medaka fish, and human PCD patients (Omran et al., 2008), supporting a conserved role for this protein in a cytoplasmic step in the assembly process. In contrast, mutations in Oda7/LRRC50 only affect outer row dynein in the alga, leading to reduced beat frequency but not complete paralysis of the flagella (Kamiya 1988), whereas mutations in the vertebrate orthologs appear to affect both outer and inner row dyneins and to completely disrupt ciliary motility in zebrafish (Sullivan-Brown et al., 2008; VanRooijen et al., 2008) and in human patients (Duquesnoy et al., 2009). To confirm whether the IFT-dependent dynein assembly mechanism defined by *oda16* mutations in *Chlamydomonas* is relevant to vertebrates, we turned to zebrafish as a useful model organism for such validation.

The role of ciliary motility in zebrafish development was first established through the selection of random mutations with developmental defects (Sun et al., 2004; Zhao and Malicki 2007; Sullivan-Brown et al., 2008), and more recently by direct knockdown of the expression of known ciliary proteins (Essner et al., 2005; Kramer-Zucker et al., 2005). Motile cilia in zebrafish embryos play well-documented roles in embryonic left-right asymmetry determination and pronephros function (Essner et al., 2005; Kramer-Zucker et al., 2005), and were recently recognized as essential to otolith formation as well; knockdown of a dynein regulatory complex subunit, which led to impaired ciliary motility, resulted in abnormal otolith formation (Colantonio et al., 2009). Asymmetry determination in zebrafish involves Kupffer's vesicle (KV), a transient spherical cavity functionally analogous to the mouse embryonic node. It has been hypothesized that a leftward flow generated by motile cilia within KV initiates asymmetrical gene expression during embryogenesis (Essner et al., 2005), and that failure to generate a directional flow within KV therefore leads to left-right asymmetry defects during later organogenesis (Bisgrove and Yost 2006).

Here we provide the first characterization of the *wdr69* gene, the zebrafish homolog of *ODA16*. We show *wdr69* is specifically expressed in organs that have motile cilia, including the pronephros, otic vesicles and KV. Using antisense morpholino oligonucleotides (MO) to knock down *wdr69* expression, we show that Oda16/Wdr69 plays an essential role in formation of otoliths in otic vesicles and in the generation of fluid flow in KV that is necessary for establishing organ laterality. Otolith and laterality defects in morphant embryos arise from disrupted ciliary motility, due to loss of outer arm dynein assembly onto

ciliary axonemes. These results indicate that the role of Oda16 in dynein assembly is conserved from *Chlamydomonas* to a vertebrate system, *Danio rerio*. It is highly likely that functions of Oda16 identified in zebrafish will extend to other vertebrate systems as well, and thus Oda16/WDR69 should be considered as a candidate locus for human PCD.

Results

Zebrafish wdr69 is only expressed in cells that assemble motile cilia

Chlamydomonas cells carrying *oda16* mutations swim with greatly reduced beat frequencies, a phenotype typical of outer arm dynein mutants in this organism (Ahmed and Mitchell 2005). The reduced assembly of outer arm dynein in these strains is due to lack of proper IFT-based transport of assembled dynein complexes from the cytoplasm into the flagellar compartment for attachment to doublet microtubules (Ahmed et al., 2008). To see if the zebrafish homolog of Oda16 serves a similar role, we first checked for the presence of homologous genes and identified a single gene in the zebrafish genome database, *wdr69*, which encodes a protein with high similarity to *Chlamydomonas* Oda16. Sequence alignments indicate that *Chlamydomonas* Oda16 shares over 70% similarity and 60% identity to its human and zebrafish homologs (Figure 1A).

To examine the expression pattern of *wdr69* in zebrafish, we performed RNA *in situ* hybridization with probes developed from a zebrafish *wdr69* cDNA clone. *wdr69* expression was detected at several stages during embryogenesis, but only within organs that make motile cilia. At 80% and 95% epiboly, expression of *wdr69* was limited to dorsal forerunner cells (Figure 1B-C), which later give rise to KV (Melby et al., 1996; Cooper and D'Amico 1996). At the 6 somite stage (SS), expression of *wdr69* was detected in KV as well as in the notochord and floorplate midline (Figure 1D-E). At 18 SS, *wdr69* was expressed in otic vesicle, pronephric duct and spinal cord, all locations where the existence of motile cilia has been previously reported (Figure 1F-G).

Wdr69 morphants develop phenotypes associated with defects in ciliary motility

To determine the role of Wdr69 in zebrafish development, we used antisense MOs to reduce *wdr69* expression. Embryos injected with control MO had normal morphology at 2 days post-fertilization (dpf) (Figure 2A), whereas embryos injected with *wdr69* MO^{AUG}, designed to block *wdr69* translation, exhibited a curled tail phenotype (Figure 2B) reminiscent of phenotypes previously associated with defects in either motility (Essner et al., 2005; Kramer-Zucker et al., 2005) or assembly (Bisgrove et al., 2005) of cilia. By 3 dpf, a portion of morphants (27%, n=92) developed kidney cysts visible by light microscopy (arrow in Figure 2C), whereas no cysts were observed in control MO embryos (n=126). In addition, *wdr69* morphants developed pericardial edema (arrowhead in Figure 2C), which can be caused by defects in either heart development or kidney function. We also examined otolith formation, since motile cilia play a role in the formation of a normal number of otoliths in zebrafish (Colantonio et al., 2009). Control MO injected embryos developed two otoliths (98%, n=90), one at the anterior end and one at the posterior end of the otic vesicle (Figure 2D). In contrast, *wdr69* MO^{AUG} morphants often developed an abnormal number of otoliths with the majority (64%, n=77) containing three otoliths, two correctly positioned and one ectopically positioned (Figure 2E).

To determine whether *wdr69* MO^{AUG} phenotypes were specific to *wdr69* knockdown, rather than due to MO off-target effects, we designed a second MO to block splicing of *wdr69* transcripts at the intron 2 - exon 3 junction (*wdr69* MO^{I2E3}). Embryos injected with *wdr69* MO^{I2E3} developed phenotypes similar to those observed in *wdr69* MO^{AUG} morphants, including a curled tail at 2 dpf (Figure 2F). The efficacy of *wdr69* MO^{I2E3} was tested by

RT-PCR. In control embryos, primers spanning exons 2-4 amplified a normally spliced fragment of *wdr69* (Figure 2G). In *wdr69* MO^{I2E3} morphants, the amount of this fragment was reduced and a smaller fragment was detected with a size equal to exon 2 plus exon 4 but lacking exon 3 (Figure 2G). Sequence analysis confirmed that exon 3 is missing in this smaller fragment, leading to a frame shift and premature stop codon. Taken together, the exclusive expression of *wdr69* in ciliated tissues and similar cilia-associated phenotypes caused by two independent *wdr69* MOs indicated these phenotypes are specific to *wdr69* depletion and that Wdr69 is required for the function of motile cilia in zebrafish.

Wdr69 is important for the establishment of left-right asymmetry

To further characterize the role of Wdr69 in cilia-mediated developmental processes, we next analyzed left-right asymmetry in *wdr69* morphants. We examined heart and gut laterality via RNA *in situ* hybridization using *cmlc2* and *foxa3* anti-sense probes, respectively. In control embryos, we observed normal looping of the heart (Figure 3A) and orientation of the gut (Figure 3D). However, the heart often showed reversed looping (Figure 3B) or failed to loop (Figure 3C) in *wdr69* MO^{AUG} morphants. Similarly, gut position in *wdr69* MO^{AUG} morphants was randomized among normal, reversed (Figure 3E) and bilateral (Figure 3F). Morphants with reversed heart looping also typically exhibited reversed gut position, which strongly indicates complete *situs inversus*. Similar heart and gut laterality defects were observed in *wdr69* MO^{I2E3} morphants. The percentage of embryos showing gut positioning as well as heart looping defects is shown in Figure 3J and reported in Table 1.

The observation of randomized organ laterality in *wdr69* morphants is consistent with a role for Wdr69 in the function of KV cilia. Motile cilia in KV generate an asymmetric fluid flow that is upstream of the earliest known left-right asymmetry in zebrafish—the left sided expression of the nodal-related gene *southpaw* (*spaw*) (Long et al., 2003). In control embryos at 18 SS, *spaw* expression was restricted to the left lateral plate mesoderm (LPM) (Figure 3G). In contrast, *wdr69* MO^{AUG} morphants displayed abnormal right and bilateral distributions of *spaw* expression in LPM (Figure 3H, I), with the majority of *wdr69* MO^{AUG} morphants showing bilateral expression (Table 1). Such randomized laterality of *spaw* expression is consistent with defects in KV cilia form or function as previously described (Essner et al., 2005; Bisgrove et al., 2005; Kramer-Zucker et al., 2005; Yamauchi et al., 2009).

Wdr69 is needed for ciliary motility and outer arm dynein assembly

To see what role *wdr69* plays in KV and other ciliated organs we first examined the length and number of motile cilia. Using acetylated tubulin immunofluorescent staining, we found that cilia were present in *wdr69* MO^{AUG} morphants and appeared similar to cilia in control embryos in KV (Figure 4A-B), the pronephric ducts (Figure 4C-D) and otic vesicles (Figure 4E-F). Measurements of cilia in KV at 6-8 SS revealed no significant difference in either length or number in *wdr69* MO^{AUG} morphants compared with control MO injected embryos (Figure 4G-H). Thus, similar to C*hlamydomonas oda16* mutants, which have normal flagellar length, Wdr69 knockdown does not affect length of motile cilia in zebrafish.

We next employed live video microscopy of ciliary motility, as seen by differential interference contrast (DIC) microscopy, and fluid flow, as detected by the motion of fluorescent beads microinjected into the KV, to determine the effects of Wdr69 knockdown on ciliary function. At 8-10 SS, KV cilia were motile and beat in a rotational pattern in control MO injected embryos (Movie 1). Consistent with previous results (Essner et al., 2005), fluorescent beads injected into KV at 8-10 SS flowed in a counterclockwise direction as visualized under DIC and fluorescent microscopy (Movie 2). In contrast, KV cilia

motility was greatly reduced in *wdr69* MO^{AUG} (Movie 3) and *wdr69* MO^{I2E3} (Movie 4) morphants. In morphant embryos, some KV cilia totally lost their motility while others retained minimal abnormal motility typified by jerky movements. Consequentially, fluorescent beads injected in *wdr69* morphants bounced uncoordinatedly and were not able form a directional flow (Movie 5). Using tracking software to follow bead paths, we found that in addition to a loss of flow directionality in *wdr69* MO^{AUG} morphants (Figure 5B) relative to controls (Figure 5A), the velocity of bead movement was significantly reduced in Wdr69 knockdown embryos (Figure 5C). Abrogation of fluid flow in KV provides an explanation for left-right asymmetry defects in *wdr69* morphant embryos.

To test whether Wdr69 is also required for cilia motility in other organs, we imaged otic vesicle cilia in live embryos. Otic vesicles contain two groups of cilia, short non-motile cilia and long motile tether cilia. Tether cilia beating is essential for normal otolith formation in the developing zebrafish ear (Colantonio et al., 2009). Video microscopy showed that unlike the fast beating tether cilia observed in control MO injected embryos (Movie 6), the motility of tether cilia was greatly impaired in *wdr69* morphants at 24 hpf (Movie 7). Thus, the need for Wdr69 to support normal motility is not limited to KV cilia.

Finally, to determine the extent of the ciliary ultrastructural defects that might be responsible for these effects on motility, we used electron microscopy. Thin sections of KV cilia in control MO injected embryos revealed the presence of typical outer dynein arms on all nine outer doublets of all cilia examined (Figure 5D), whereas cilia from *wdr69* MO^{AUG} morphants consistently displayed greatly reduced numbers of outer dynein arms (Figure 5E), similar to reductions reported in *Chlamydomonas oda16* axonemes (Ahmed and Mitchell 2005). Electron density in the inner row dynein region did not appear altered, but further analysis will be needed to rule out the possibility of a loss of some inner row dynein species. Interestingly, we observed two different groups of KV cilia, those with (9+2 arrangement) or without (9+0) central pair microtubules, in both control and *wdr69* MO^{AUG} morphant embryos. Similar variability in the appearance of central pair microtubules has been reported previously for nodal cilia in mouse (Caspary et al., 2007) and rabbit (Feistel and Blum 2006).

Discussion

Defects in motile cilia have been linked in mammals to developmental abnormalities in visceral organs (due to heterotaxia) and, at least in rodents, in the brain (due to hydrocephalus). In human PCD patients, ciliary motility defects correlate most frequently with mutations in axonemal outer row dynein subunits such as DNAH5, DNAI1 and DNAI2 (Guichard et al., 2001; Olbrich et al., 2002; Loges et al., 2008). We have recently shown that similar dynein assembly defects can result from mutations in proteins needed for cytoplasmic pre-assembly of axonemal dyneins, such as PF13/Ktu (Omran et al., 2008) and Oda7/LRRC50 (Duquesnoy et al., 2009), however, both of these proteins are also needed for assembly of one or more inner row dynein in vertebrates. Here, we show that defects related to loss of Wdr69 in zebrafish disrupt assembly of outer row dyneins. Wdr69, like Ktu and LRRC50, is a protein needed for dynein assembly rather than a dynein subunit, but unlike Ktu and LRRC50 mutations, loss of Wdr69 does not appear to alter inner row dynein assembly. The zebrafish phenotypes in *wdr69* morphants are consistent those seen previously in embryos with outer row dynein heavy chain defects (Essner et al., 2005; Kramer-Zucker et al., 2005), including curly tail, formation of pronephric cysts, and left-right asymmetry defects. By electron microscopy only outer row dyneins appeared specifically depleted from KV cilia of *wdr69* morphants (Fig. 5E), without other obvious changes in ciliary length, number, distribution or ultrastructure. Thus the role of Oda16/Wdr69 appears to be identical in a vertebrate (zebrafish) and an alga (*Chlamydomonas*).

A conserved function for Oda16/Wdr69 as a cargo-specific assembly factor in organisms as distantly related as fish and algae suggests that this function evolved prior to the divergence of all existing eukaryotes from a common ancestor, and has not changed in any obvious way over the intervening ca. one billion years (Keeling et al., 2005). Consistent with this interpretation, both the single IFT subunit that has been shown to interact directly with Oda16/Wdr69, IFT46 (Ahmed et al., 2008), and subunits of the outer row dynein complex itself that is transported by Oda16 (including both heavy chains and intermediate chains) (Wickstead and Gull 2007; Wilkes et al., 2008) appear to have existed prior to eukaryotic radiation. Although outer row dynein intermediate and heavy chain subunits diversified further in vertebrates through gene duplications, organisms that use outer row dyneins have retained just one Wdr69 homolog, which is likely to perform the same function in IFT-based transport of outer row dyneins in all cell types that use motile cilia. The WDR69 gene should therefore be considered as a candidate in screens for human PCD loci. Recent success at *in vitro* rescue of ciliary motility by transfer of a dynein intermediate chain gene into respiratory epithelial cells from a PCD patient (Chhin et al., 2009) points to the potential for correction of such genetic defects.

Experimental Procedures

Zebrafish

AB wild type zebrafish were obtained from the Zebrafish International Resource Center (ZIRC) and maintained as previously described (Westerfield 1995). Embryos were obtained from natural matings and staged as described in (Kimmel et al., 1995).

RNA *in situ* hybridization

A zebrafish *wdr69* cDNA clone was purchased from Open Biosystems (clone ID 892486) and subcloned into the pCR2.1 vector (Invitrogen). The pCR2.1-wdr69 construct was linearized with Not I and served as template for the synthesis of antisense probes with SP6 RNA polymerase. Antisense probes for *wdr69*, *southpaw* (*spaw*), *cardiac myosin light chain 2* (*cmlc2*), *forkhead box a3* (*foxa3*) were generated using a DIG RNA labeling kit (Roche). RNA probes were purified using Micro Bio-Spin Chromatography Columns (Bio-Rad). If necessary, embryos were treated with 1-phenyl 2-thiourea (PTU) at 24 hpf to inhibit melanin synthesis. Embryos were then fixed at the stages indicated with 4% paraformaldehyde in sucrose buffer overnight at 4 degrees. Following dehydration and rehydration, embryos were digested with proteinase K and pre-hybridized in hybridization buffer for 4 hours at 67 degrees. Embryos were then incubated with RNA probes diluted in hybridization buffer (1μg/ml) overnight at 67 degrees. Embryos were then washed and incubated overnight with pre-absorbed anti-digoxigenin alkaline phosphatase-conjugated antibodies (Roche) at a concentration of 1:1000. Following washes, embryos were stained using NBT and BCIP (Roche). Stained embryos were fixed in 4% paraformaldehyde and cleared in 70% glycerol. Images were taken using a Zeiss Axiocam MRc digital camera on a Zeiss Discovery v12 stereo microscope and processed with Axiovision (Zeiss) and Photoshop (Adobe) software.

Morpholino injection

Antisense morpholino oligonucleotides (MO) directed against the zebrafish *wdr69* start codon to block translation (*wdr69* MO^{AUG}: 5′-TGTGCATCCGTTTCAGTCTCATCAC-3′) and the intron 2-exon 3 splice acceptor site to block mRNA splicing (*wdr69* MO^{I2E3}: 5′-ATCAGTCCTGGAGGAGAAATATAGA-3′) were synthesized by Gene Tools, LLC. A standard negative control MO was also purchased from Gene Tools. To knock down zebrafish *wdr69* expression, embryos were injected with either 1.5 ng *wdr69* MO^{AUG} or 2.5 ng *wdr69* MO^{I2E3} at the 1–2 cell stages.

RT-PCR

Total RNA was isolated from embryos using TRIzol Reagent (Invitrogen) and used to produce cDNA via the Superscript First-Strand Synthesis System (Ambion). The resulting cDNAs were used as templates to PCR amplify a small region of the *wdr69* gene spanning exons 2-4 using a forward primer in exon 2 (Splicing MO-F: 5′-gaatttttctagactatgag-3′) and a reverse primer in exon 4 (Splicing MO-R: 5′-caagatcctgatttattgaagg-3′). Primers in the *β-actin* gene (Forward 105: 5′-GGTATGGGACAGAAAGACAG-3′ and Reverse 106: 5′-AGAGTCCATCACGATACCAG-3′) were used as positive controls.

Whole-mount immunohistochemistry

Embryos fixed in 4% paraformaldehyde were dechorionated and incubated in blocking solution (PBS containing 5% sheep serum, 1% bovine serum albumin, 1% DMSO and 0.1% triton X) for 1 h and then incubated with primary antibody (mouse anti-acetylated tubulin antibody, Sigma T-6793) overnight. Embryos were then washed and incubated with secondary antibody (goat anti-mouse Alexa Fluor 488, Molecular Probes) overnight. Embryos were mounted in Slow Fade Reagent (Invitrogen) and visualized using a 63× objective on a Zeiss AxioImager M1 microscope. Images were captured with a Zeiss Axiocam HSm digital camera and processed using Axiovision software. All Z-series images were assembled using Image J (NIH) and processed using Photoshop (Adobe) software. Cilium length was measured using ImageJ.

Video microscopy of cilia and fluorescent beads

For imaging cilia in KV and otic vesicles, or fluorescent beads (Polysciences, Inc.) injected into the KV lumen at 6-8 SS (Essner et al., 2005), live zebrafish embryos were treated with 0.4% tricaine (MS-222) and embedded in 1% low melting agarose. Ciliary motility or bead movement was captured using a Zeiss Axiocam high-speed monochromatic camera mounted on a Zeiss AxioImager M1 microscope with a 63× water-dipping objective. Movies were generated using Axiovision and Quicktime (Apple) software. Bead velocity was determined using Axiovision tracking software.

Electron Microscopy

Dechorionated embryos were fixed in 2% formaldehyde, 2% glutaraldehyde, 0.5% tannic acid in 0.1 M sodium cacodylate buffer, pH 8.0 for 1 hr at RT, and post-fixed in 1% OsO4 in 0.1 M sodium cacodylate for 30 min at RT prior to dehydration and infiltration with embedding resin. Yolk was dissected away from embryos after infiltration but prior to resin polymerization. Thin sections were stained with uranyl acetate and lead citrate, and observed on a JEOL 100 C electron microscope.

Supplementary Material

Refer to Web version on PubMed Central for supplementary material.

Acknowledgments

The authors would like to thank Fiona Foley and Masako Nakatsugawa for technical assistance.

Supported by NIGMS:044228 to DRM

Reference List

Ahmed NT, Gao C, Lucker BF, Cole DG, Mitchell DR. ODA16 aids axonemal outer row dynein assembly through an interaction with the intraflagellar transport machinery. J Cell Biol. 2008; 183:313–322. [PubMed: 18852297]

Ahmed NT, Mitchell DR. ODA16p, a Chlamydomonas flagellar protein needed for dynein assembly. Mol Biol Cell. 2005; 16:5004–5012. [PubMed: 16093345]

Bisgrove BW, Snarr BS, Emrazian A, Yost HJ. Polaris and Polycystin-2 in dorsal forerunner cells and Kupffer's vesicle are required for specification of the zebrafish left-right axis. Dev Biol. 2005; 287:274–288. [PubMed: 16216239]

Bisgrove BW, Yost HJ. The roles of cilia in developmental disorders and disease. Development. 2006; 133:4131–4143. [PubMed: 17021045]

Carlen B, Stenram U. Primary ciliary dyskinesia: a review. Ultrastruct Pathol. 2005; 29:217–220. [PubMed: 16036877]

Caspary T, Larkins CE, Anderson KV. The graded response to Sonic Hedgehog depends on cilia architecture. Dev Cell. 2007; 12:767–778. [PubMed: 17488627]

Chhin B, Negre D, Merrot O, Pham J, Tourneur Y, Ressnikoff D, Jaspers M, Jorissen M, Cosset FL, Bouvagnet P. Ciliary beating recovery in deficient human airway epithelial cells after lentivirus ex vivo gene therapy. PLoS Genet. 2009; 5:e1000422. [PubMed: 19300481]

Colantonio JR, Vermot J, Wu D, Langenbacher AD, Fraser S, Chen JN, Hill KL. The dynein regulatory complex is required for ciliary motility and otolith biogenesis in the inner ear. Nature. 2009; 457:205–209. [PubMed: 19043402]

Cooper MS, D'Amico LA. A cluster of noninvoluting endocytic cells at the margin of the zebrafish blastoderm marks the site of embryonic shield formation. Dev Biol. 1996; 180:184–198. [PubMed: 8948584]

Duquesnoy P, Escudier E, Vincensini L, Freshour J, Bridoux AM, Coste A, Deschildre A, de BJ, Legendre M, Montantin G, Tenreiro H, Vojtek AM, Loussert C, Clement A, Escalier D, Bastin P, Mitchell DR, Amselem S. Loss-of-Function Mutations in the Human Ortholog of Chlamydomonas reinhardtii ODA7 Disrupt Dynein Arm Assembly and Cause Primary Ciliary Dyskinesia. Am J Hum Genet. 2009; 85:890–896. [PubMed: 19944405]

Eley L, Yates LM, Goodship JA. Cilia and disease. Curr Opin Genet Dev. 2005; 15:308–314. [PubMed: 15917207]

Essner JJ, Amack JD, Nyholm MK, Harris EB, Yost J. Kupffer's vesicle is a ciliated organ of asymmetry in the zebrafish embryo that initiates left-right development of the brain, heart and gut. Development. 2005; 132:1247–1260. [PubMed: 15716348]

Feistel K, Blum M. Three types of cilia including a novel 9+4 axoneme on the notochordal plate of the rabbit embryo. Dev Dyn. 2006; 235:3348–3358. [PubMed: 17061268]

Guichard C, Harricane MC, Lafitte JJ, Godard P, Zaegel M, Tack V, Lalau G, Bouvagnet P. Axonemal dynein intermediate-chain gene (*DNAI1*) mutations result in situs inversus and primary ciliary dyskinesia (Kartagener syndrome). Am J Hum Genet. 2001; 68:1030–1035. [PubMed: 11231901]

Kamiya R. Mutations at twelve independent loci result in absence of outer dynein arms in *Chylamydomonas reinhardtii*. J Cell Biol. 1988; 107:2253–2258. [PubMed: 2974040]

Keeling PJ, Burger G, Durnford DG, Lang BF, Lee RW, Pearlman RE, Roger AJ, Gray MW. The tree of eukaryotes. Trends Ecol Evol. 2005; 20:670–676. [PubMed: 16701456]

Kimmel CB, Ballard WW, Kimmel SR, Ullmann B, Schilling TF. Stages of embryonic development of the zebrafish. Dev Dyn. 1995; 203:253–310. [PubMed: 8589427]

Kramer-Zucker AG, Olale F, Haycraft CJ, Yoder BK, Schier AF, Drummond IA. Cilia-driven fluid flow in the zebrafish pronephros, brain and Kupffer's vesicle is required for normal organogenesis. Development. 2005; 132:1907–1921. [PubMed: 15790966]

Loges NT, Olbrich H, Fenske L, Mussaffi H, Horvath J, Fliegauf M, Kuhl H, Baktai G, Peterffy E, Chodhari R, Chung EM, Rutman A, O'Callaghan C, Blau H, Tiszlavicz L, Voelkel K, Witt M, Zietkiewicz E, Neesen J, Reinhardt R, Mitchison HM, Omran H. DNAI2 mutations cause primary ciliary dyskinesia with defects in the outer dynein arm. Am J Hum Genet. 2008; 83:547–558. [PubMed: 18950741]

Long S, Ahmad N, Rebagliati M. The zebrafish nodal-related gene southpaw is required for visceral and diencephalic left-right asymmetry. Development. 2003; 130:2303–2316. [PubMed: 12702646]

Melby AE, Warga RM, Kimmel CB. Specification of cell fates at the dorsal margin of the zebrafish gastrula. Development. 1996; 122:2225–2237. [PubMed: 8681803]

Nonaka S, Tanaka Y, Okada Y, Takeda S, Harada A, Kanai Y, Kido M, Hirokawa N. Randomization of left-right asymmetry due to loss of nodal cilia generating leftward flow of extraembryonic fluid in mice lacking KIF3B motor protein. Cell. 1998; 95:829–837. [PubMed: 9865700]

Okada Y, Takeda S, Tanaka Y, Belmonte JC, Hirokawa N. Mechanism of nodal flow: a conserved symmetry breaking event in left-right axis determination. Cell. 2005; 121:633–644. [PubMed: 15907475]

Olbrich H, Häffner K, Kispert A, Völkel A, Volz A, Sasmaz G, Reinhardt R, Hennig S, Lehrach H, Konietzko N, Zariwala M, Noone PG, Knowles M, Mitchison HM, Meeks M, Chung EMK, Hildebrandt F, Sudbrak R, Omran H. Mutations in *DNAH5* cause primary ciliary dyskinesia and randomization of left-right and asymmetry. Nature Genet. 2002; 30:143–144. [PubMed: 11788826]

Omran H, Kobayashi D, Olbrich H, Tsukahara T, Loges NT, Hagiwara H, Zhang Q, Leblond G, O'Toole E, Hara C, Mizuno H, Kawano H, Fliegauf M, Yagi T, Koshida S, Miyawaki A, Zentgraf H, Seithe H, Reinhardt R, Watanabe Y, Kamiya R, Mitchell DR, Takeda H. Ktu/PF13 is required for cytoplasmic pre-assembly of axonemal dyneins. Nature. 2008; 456:611–616. [PubMed: 19052621]

Pazour GJ, Dickert BL, Vucica Y, Seeley ES, Rosenbaum JL, Witman GB, Cole DG. Chlamydomonas IFT88 and its mouse homologue, polycystic kidney disease gene *Tg737*, are required for assembly of cilia and flagella. J Cell Biol. 2000; 151:709–718. [PubMed: 11062270]

Sullivan-Brown J, Schottenfeld J, Okabe N, Hostetter CL, Serluca FC, Thiberge SY, Burdine RD. Zebrafish mutations affecting cilia motility share similar cystic phenotypes and suggest a mechanism of cyst formation that differs from pkd2 morphants. Dev Biol. 2008; 314:261–275. [PubMed: 18178183]

Sun ZX, Amsterdam A, Pazour GJ, Cole DG, Miller MS, Hopkins N. A genetic screen in zebrafish identifies cilia genes as a principal cause of cystic kidney. Development. 2004; 131:4085–4093. [PubMed: 15269167]

VanRooijen E, Giles RH, Voest EE, VanRooijen C, Schulte-Merker S, VanEeden FJ. LRRC50, a conserved ciliary protein implicated in polycystic kidney disease. J Am Soc Nephrol. 2008; 19:1128–1138. [PubMed: 18385425]

Westerfield, M. The Zebrafish Book. Eugene: University of Oregon Press; 1995.

Wickstead B, Gull K. Dyneins across eukaryotes: a comparative genomic analysis. Traffic. 2007; 8:1708–1721. [PubMed: 17897317]

Wilkes DE, Watson HE, Mitchell DR, Asai DJ. Twenty-five dyneins in Tetrahymena: A re-examination of the multidynein hypothesis. Cell Motil Cytoskeleton. 2008; 65:342–351. [PubMed: 18300275]

Yamauchi H, Miyakawa N, Miyake A, Itoh N. Fgf4 is required for left-right patterning of visceral organs in zebrafish. Dev Biol. 2009; 332:177–185. [PubMed: 19481538]

Zhao C, Malicki J. Genetic defects of pronephric cilia in zebrafish. Mech Dev. 2007; 124:605–616. [PubMed: 17576052]

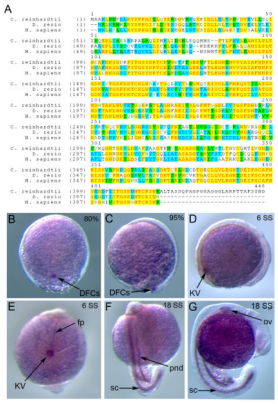

Figure 1. Zebrafish *wdr69* is expressed in cells that assemble motile cilia

(A) Protein sequence alignment of Oda16 homologs from *Chlamydomonas reinhardtii*, *Danio renio* and *Homo sapiens*. Yellow color highlights conserved residues among the three species, blue color highlights residues conserved in two species and green color highlights conservative replacements. (B-G) RNA *in situ* hybridizations detecting *wdr69* expression during early zebrafish development. At the 80% (B) and 95% (C) epiboly stages, *wdr69* is expressed exclusively in dorsal forerunner cells (DFCs). At the 6 somite stage (SS), *wdr69* is expressed in Kupffer's vesicle (KV) (D, E) and the floorplate (fp) of the neural tube (E). At 18 SS, *wdr69* is expressed in the spinal cord (sc), pronephric ducts (pnd) (F) and otic vesicle (ov) (G).

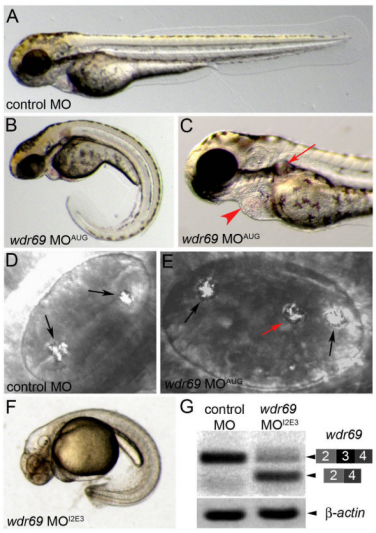

Figure 2. *wdr69* MO knockdown embryos develop phenotypes associated with defects in ciliary motility

(A-C) Live embryos at 2 days post fertilization (dpf). Control MO injected embryos exhibited normal morphology (A), whereas *wdr69* MO^{AUG} morphant embryos developed phenotypes associated with cilia defects, including a curled tail (B), kidney cysts (arrow in C) and pericardial edema (arrowhead in C). (D-E) Otoliths in otic vesicles at 2 dpf. Control MO injected embryos developed two correctly positioned otoliths (arrows in D). *wdr69* MO^{AUG} morphants often developed a third ectopically positioned otolith (red arrow in E). (F) *wdr69* MO^{I2E3} morphants developed the same phenotypes as *wdr69* MO^{AUG} morphants (this embryo was treated with PTU to inhibit melanin biosythesis for RNA *in situ* analysis). (G) RT-PCR analysis shows *wdr69* MO^{I2E3} causes mis-splicing of *wdr69* transcripts. A normally spliced cDNA containing exons 2-4 was detected in control MO injected embryos. The level of this cDNA was reduced in *wdr69* MO^{I2E3} morphants and a smaller fragment lacking exon 3 was observed in *wdr69* MO^{I2E3} morphants. *β-actin* was amplified as a loading control.

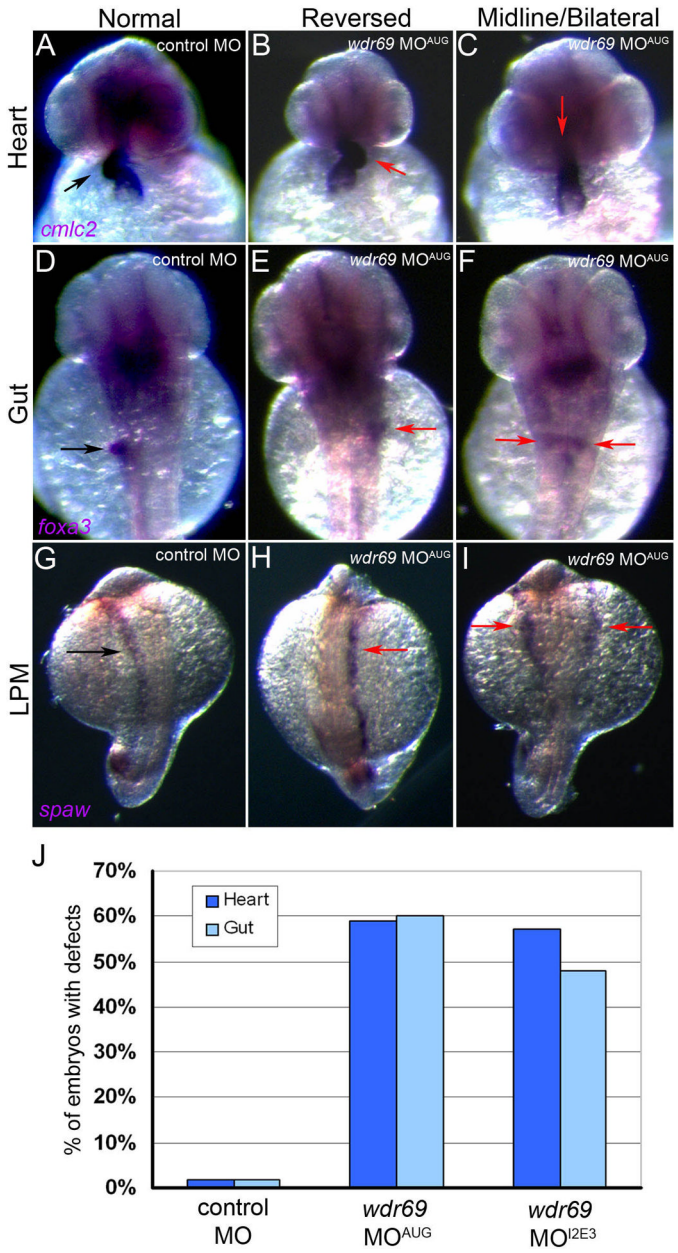

Figure 3. Wdr69 is important for the establishment of left-right asymmetry

(A-F) Analysis of organ left-right asymmetry by RNA *in situ* hybridizations using the heart marker *cmlc2* (A-C) and gut marker *foxa3* (D-F). Control morphants showed normal rightward looping of the heart (arrow in A) and left-sided orientation of the liver (arrow in D). In *wdr69* MO^{AUG} morphants, heart looping was often reversed (arrow in B) or linear along the midline (arrow in C). Similarly, liver position in *wdr69* MO^{AUG} morphants was frequently reversed (arrow in E) or bilateral (arrows in F). (G-I) RNA *in situ* hybridizations detecting *southpaw* (*spaw*) expression in lateral plate mesoderm (LPM) at 18 SS. (G). *spaw* expression was restricted to left LPM cells in control morphants (arrow in G), whereas *wdr69* MO^{AUG} morphants displayed abnormal right (arrow in H) and bilateral (arrows in I) distributions of *spaw* expression. (J) The percentage of embryos injected with control MO

(n=130), *wdr69* MO^{AUG} (n=67) or *wdr69* MO^{I2E3} (n=75) showing laterality defects in the heart and gut (see also Table 1).

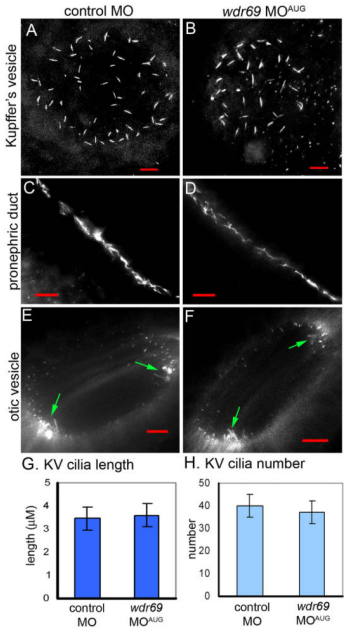

Figure 4. Cilia length and number is not changed in *wdr69* morphants

(A-F) Cilia were visualized by immunofluorescent staining with acetylated tubulin antibodies. Cilia in embryos injected with *wdr69* MO^{AUG} appeared similar to cilia injected with control MO in Kupffer's vesicle (A-B), pronephric ducts (C-D) and otic vesicles (arrows in E-F point to motile tether cilia). All red scale bars represent 10 μM. (G-H) Measurements of KV cilia at 6-8 SS showed no significant differences in the average length (G) or number (H) between *wdr69* MO^{AUG} (n=17) and control (n=21) morphants. Error bars=one standard deviation.

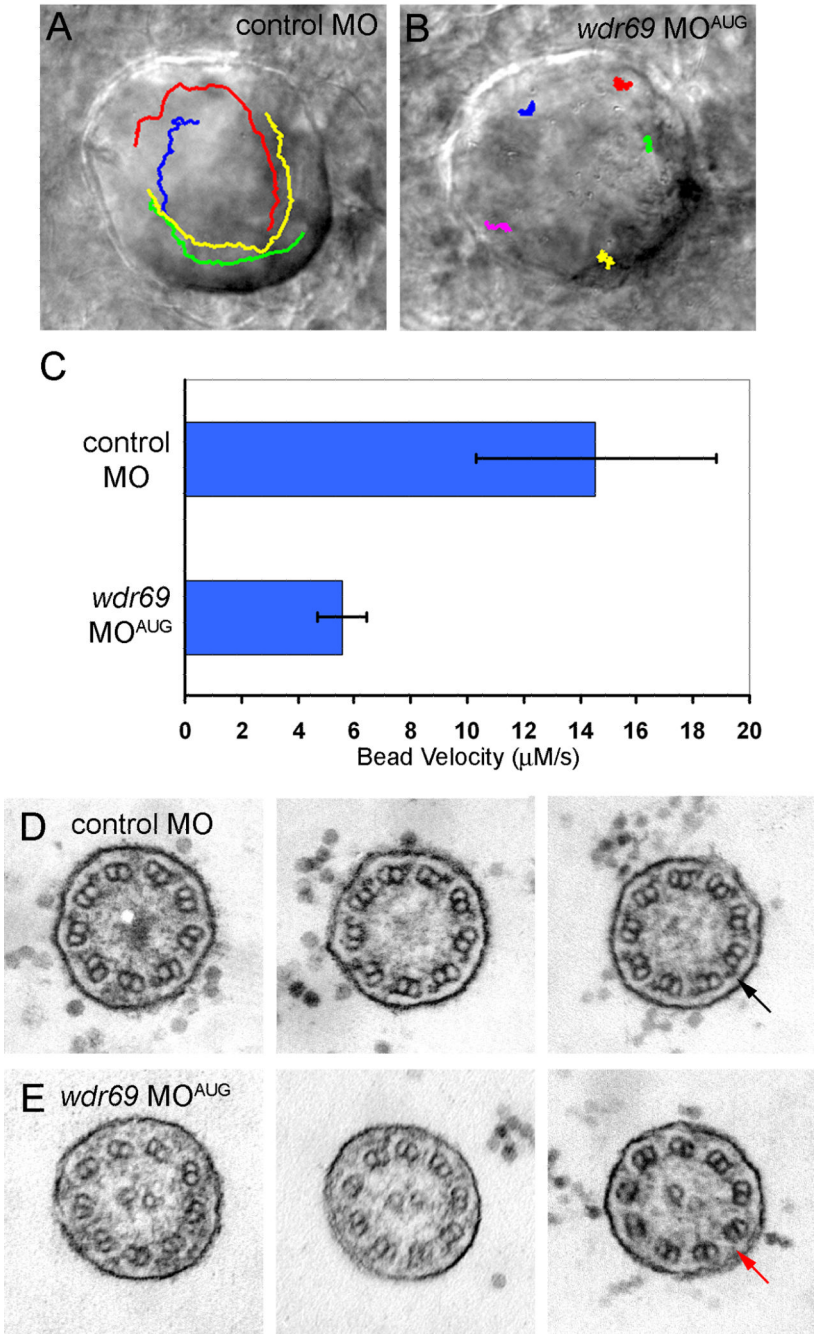

Figure 5. Wdr69 is needed for ciliary motility and outer arm dynein assembly

(A-B) Tracking software was used to follow the flow of fluorescent beads injected into KV of live embryos. Tracks are superimposed on images of KV. In control morphants (A), beads flowed in a circular counterclockwise direction. This directional flow was lost in *wdr69* MO^{AUG} morphants (B), where beads bounced around randomly. (C) Velocity of bead movement was significantly reduced in *wdr69* knockdown embryos (n=25 beads from 5 embryos) relative to controls (n=28 beads from 6 embryos). Error bars=one standard deviation. (D-E) Electron microscopy of KV cilia. In control MO injected embryos (D), typical outer dynein arms (arrow in D) were present on all nine outer doublets of all cilia

examined. In contrast, KV cilia from *wdr69* MO^{AUG} morphants displayed greatly reduced numbers of outer dynein arms (E).

Table 1

WDR69 Morphant Embryos have Laterality Defects

MARKER	EMBRYOS	*N*	NORMAL	REVERSED	BILATERAL	ABSENT
CMLC2 (HEART)	CONTROL MO	*130*	98%	1%	1%	--
	WDR69 MO^{AUG}	*67*	41%	52%	7%	--
	WDR69 MO^{I2E3}	*75*	43%	53%	4%	--
FOXA3 (GUT)	CONTROL MO	*130*	98%	1%	1%	--
	WDR69 MO^{AUG}	*67*	40%	45%	15%	--
	WDR69 MO^{I2E3}	*75*	52%	48%	0%	--
SPAW (LPM)	CONTROL MO	*56*	91%	0%	5%	4%
	WDR69 MO^{AUG}	*62*	21%	16%	55%	8%